

MODELING THE IMPACTS OF PETROPHYSICAL AND TEXTURAL PARAMETERS ON DISSOLUTION OF CARBONATE ROCKS AT 25°C, 50°C, AND 75°C

Spariharijaona Andriamihaja^{1*}, E. Padmanabhan¹, Joel Ben-Awuah² and Rajalingam Sokkalingam³

¹ *Department of Geosciences, Faculty of Geosciences and Petroleum Engineering Universiti Teknologi PETRONAS, 32610 Tronoh, Malaysia*

² *Department of Petroleum Engineering, Faculty of Engineering and Built Technology, UCSI University, No. 1 Jalan Menara Gading, UCSI Heights, Taman Connaught, 56000 Kuala Lumpur, Malaysia*

³ *Fundamental and Applied Science Department, Universiti Teknologi PETRONAS, Bander Seri Iskandar, 32610 Tronoh, Perak Darul Ridzuan, Malaysia.*

Received May 23, 2016; Accepted June 22, 2016

Abstract

Carbonate rocks react easily with the surrounding environment, especially in acidic environment. This property leads to very complex and heterogeneous fabric but can also be an important advantage in EOR method and CO₂ sequestration. Extensive studies have been carried on carbonate dissolution but the dissolution response of different microfacies at different temperature is still unpredictable and challenging to predict. The aim of this study is to develop predictive dissolution models for different carbonate microfacies at 25°C, 50°C and 75°C, under controlled conditions. The models are developed as a function of time of dissolution, pore-filling carbonate crystal size, porosity and permeability. The results show that as a function of only time, the dissolution models are described by log linear function where the dissolution rate increases as the temperature increases. The other developed dissolution models show that time and porosity have positive impact on dissolution whereas crystal size slows the dissolution. Based on the models, permeability appears to have no impact on dissolution. The predicted results obtained from the different models are in good agreement with the measured experimental data.

Keywords: Carbonate Microfacies; Dissolution Model, Porosity, Permeability.

1. Introduction

Carbonates are chemically unstable rocks and can easily react with the surrounding environment. Its ability to dissolve easily contributes to the heterogeneity of the rock fabric and the pore system complexities. However, this property can also be useful in selection of appropriate EOR (Enhanced Oil Recovery) methods for carbonate reservoirs, such as fracture acidizing. Therefore, in reservoir characterization, having a better understanding of dissolution kinetic of carbonate rocks will help to understand the pore systems and the rock fabric behavior in acidic environment. Several authors have studied extensively the mechanism of dissolution kinetics of carbonate rocks and the factors controlling it [1-4]. The effect of controlling laboratory factors have also been extensively studied. Letterman [3] studied the effect of temperature on dissolution rate and stated that the dissolution rate increased with increasing temperature. Dolgaleva [5] carried out research on the effect of pH on dissolution and concluded that the dissolution rate is determined by the different adsorption of the species and the characteristic "Acid -base" of the calcite dissolved in the solution.

Despite the extensive studies on carbonate dissolution, the prediction of the dissolution kinetic of specific carbonate microfacies still remains a challenge. The objective of this study, therefore, is to develop dissolution kinetic model of different microfacies at various tempe-

ratitudes and to propose predictive models as a function of petrophysical and textural parameters for each microfacies.

2. Materials and methods

Three microfacies were studied in this paper. The applied method was subdivided in two main parts. The first part consists of characterizing the microfacies based on petrographic studies using thin sections and scanning electron microscopy (SEM). These microfacies are then classified based on texture, grain types, matrix, and pore types using the Dunham classification.

The second part of the methodology is the experimental dissolution study. The sample is dissolved within a reactor chamber filled by three liters of 0.1 molar diluted HCl. The reactor consists of: (1) constant continuous rotating stirrer at 120 rpm; (2) heater automatically controlled by thermo-couple with the temperature set at 25°C, 50°C and 75°C; (3) auto-titrator that maintains the pH of the solution at 1.2 during the experiment. At every 10 min of dissolution, solution sample is collected and then analyzed by ICP -EOS in order to determine the concentration $[Ca^{2+}]$ released during the dissolution experiment.

A total of 22 samples were analyzed to define the dissolution models. The mean dissolution rate for each microfacies at different temperatures was then deduced from the variation of $[Ca^{2+}]$ during the experiment. Stepwise multiple regression analysis was used to determine the best model for each microfacies and at different temperatures.

3. Results and discussion

3.1. Microfacies description

3.1.1. Moldic muddy – wackestone (MMW)

The moldic muddy wackestone (MMW) microfacies is mud-supported, with some sparse individual bioclasts (mainly red algae). Other skeletal grains have been identified such as foraminifera (nummulites) and echinoderms. Some of these grains have been broken and replaced by micrite cements (Figure 1a).

The matrix is composed of two cement fabric types. The first cement fabric which is microcrystalline cement represents more than 56% of the entire microfacies components. It is more or less homogeneous, with light to dark microcrystals. The crystal shape is mainly anhedral (Figure 1b). The crystallization fabric of this micrite cement is inequigranular, xenotopic fabrics. The crystal sizes vary from 0.7 μm to 4.93 μm , with mean of 2.3 μm and a standard deviation of 0.97 (std: 0.97). The crystal size distribution shows a normal distribution with skewness of 0.65 and kurtosis of 0.048.

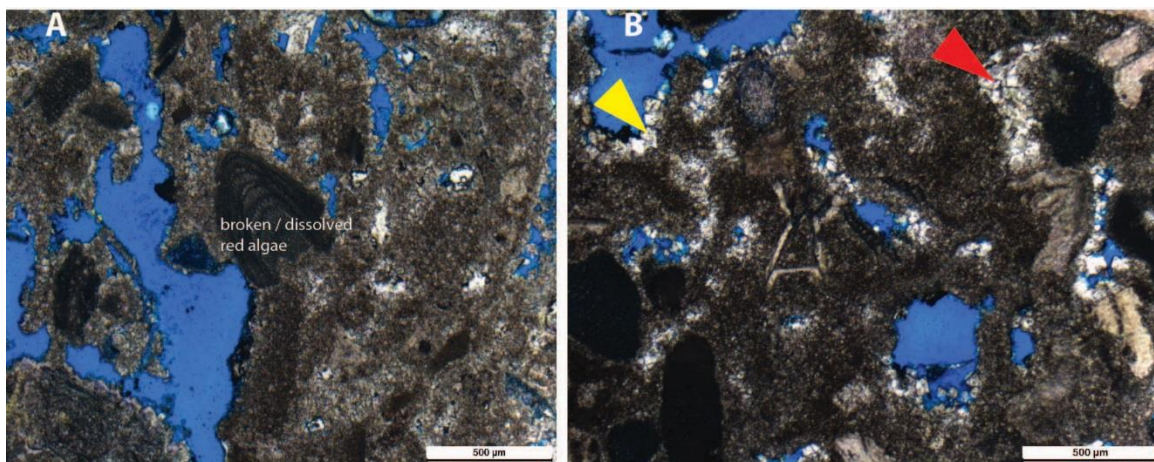


Figure 1. A- Broken or dissolved red algae, and replaced by micrite; B-Photomicrograph showing dogtooth cement at the pore edges (yellow arrow) and drusy cement type filling the pores (red arrow).

The second cement fabric is the microsparite drusy mosaic cement formed by two cement types. The first cement type is dogtooth cement. It shows sharply pointed crystal towards the pore center and occurs only at the edge of pore partially plugged. It also grows perpendicularly to the substrate (micrite or grains). The second cement type is drusy cement. This cement completely plugs pores and the crystal size increases towards the center (Figure 1b). At the pore wall, the mean size of the crystal is 51.6 μm (std: 24.5), whereas, toward the center, it is 107.2 μm , with (std: 51.7). This cement exhibits inequigranular, and xenotopic to hypodiotopic crystallization fabric.

This microfacies shows large moldic vuggy pores derived mainly from dissolution of the skeletal grains and also some intrafossil pores. In many cases, these pores are filled by cement which is an effect of recrystallization. The porosity varies widely from 8% to 24% and the permeability from 1.39mD to 26mD.

3.1.2. Boundstone (BDST)

The grains in the boundstone microfacies (BDST) were bounded together at the time of deposition (Figure 2a). However, individual skeletal grains such as red algae have been recognized. These bioclasts represent 50.4% of the sample.

Within this microfacies, there is no microcrystalline cement. There is only one cement type which is the drusy cement forming a drusy mosaic fabric. The crystal shape of this cement varies from anhedral to subhedral (Figure 2b). The crystal size ranges from 8.32 μm to 63.88 μm , with a mean of 31.26 μm (std: 13.38). The crystal size distribution shows a skewness of 0.48 and kurtosis of -0.59. The matrix constitutes 20.4% of the rock.

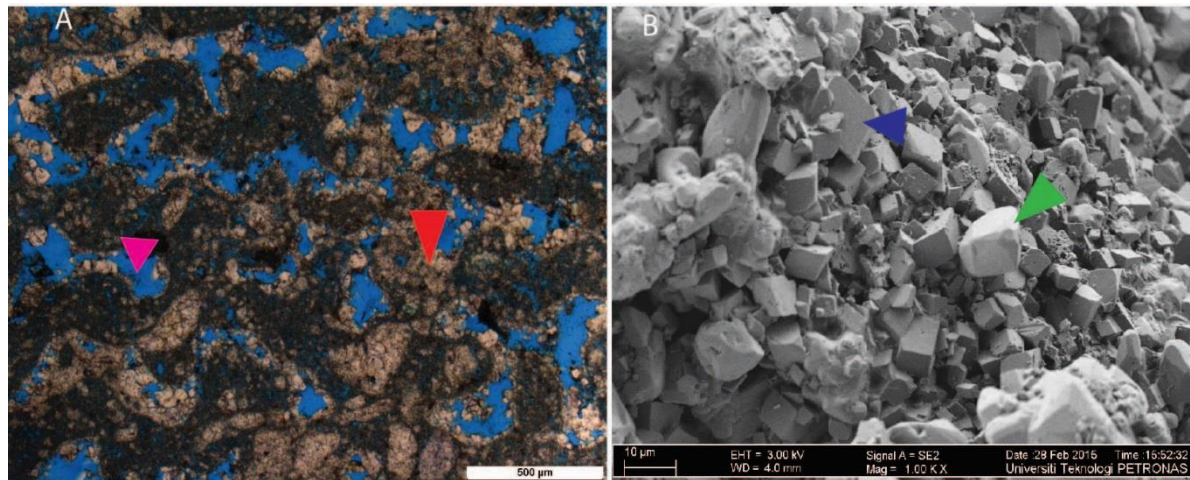


Figure 2. A- Micrograph showing grains bounded together, microsparite cement forming granular mosaic cement fabric (red arrow), intergranular (pink arrow), intrafossil, intercrystalline pore, and microfracture pores; B- Euhedral (blue arrow) to subhedral (green arrow) calcite crystal forming the drusy cement fabric.

The pores are very well connected and dominated by intergranular and intercrystalline pores. Some minor intrafossil and microfracture pores are also identified. This microfacies shows excellent porosity and permeability varying from 29.2% to 36% and 738.36mD to 2347.73mD respectively.

3.1.3. Grainstone (GRST)

Lack of carbonate mud is one of the main characteristics of this microfacies (Figure 3a). All the grains are skeletal grains and the most dominant grains are the red algae and foraminiferas (nummulites, miliolids, and few globotruncana). This microfacies is also composed of echinoderms. Some of these fossils are partially broken and then replaced by cements.

The matrix is mainly composed by micro-sparite granular cement, filling the space between the grains and also by minor dogtooth cement type (Figure 3b). This cement forms

granular cement fabric and represents 45.8% to 59.4%. The crystal shapes of these cement are mainly anhedral to subhedral and developed an inequigranular fabric. The crystal size varies from 5.25µm to 32.01 µm with a mean of 10.24 µm (std: 4.2). The skewness and the kurtosis of the crystal size distribution are 2.22 and 7.24 respectively.

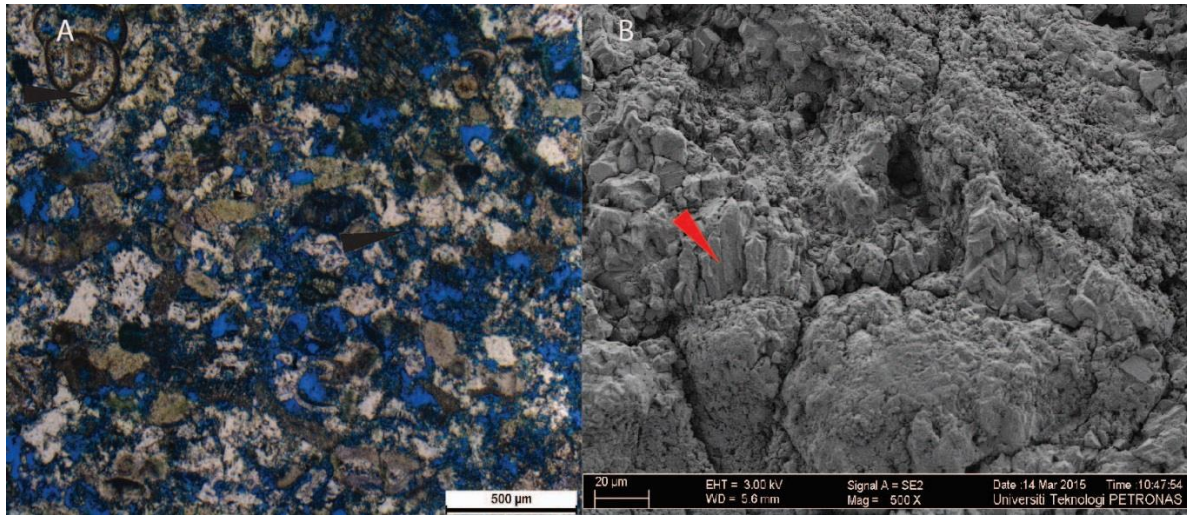


Figure 3. A- Photomicrograph showing grainstone texture with microsparite to sparite granular filling the intergranular and Intrafossil pores (black); B- Dogtooth cement (red arrow) growing perpendicular to the substrate (grains)

The pores within this facies are dominated by intergranular and intercrystalline pores. Some few micro intrafossil pores are also noted. The facies shows porosity varying from 17% to 21%. However, the permeability is relatively low (2.76mD to 4.58mD) due to the presence of high amount granular cement filling the pores.

3.2. Dissolution kinetic modeling

At 25°C, 50 °C and 75 °C, and far from equilibrium, the dissolution kinetics of the three microfacies are described by log-linear function (eq.1) with R^2 varying from 0.85 to 0.99. This indicates strong correlation between the predicted and measured dissolution rates. The general equation model is expressed as:

$$[Ca^{2+}] = m \ln t + p \tag{1}$$

The mean dissolution model is therefore defined by the slope of dissolution curve which is the dissolution rate and the intercept which is defined as the initial amount of Ca released. The parameters defining the dissolution model of each microfacies at different temperatures are presented in table 1.

Table1. Parameters defining dissolution model for different microfacies at 75°C, 50°C, and 25°C

Facies	Temp (°C)	m	p	R^2
Wackestone	75	4.65	1.07	0.94
	50	3.89	-0.5	0.85
	25	3.66	1.12	0.94
Boundstone	75	5.03	4.58	0.92
	50	5.01	1.2	0.93
	25	3.95	2.72	0.97
Grainstone	75	4.17	3.1	0.99
	50	4.05	0.57	0.91
	25	3.65	1.25	0.95

The dissolution model is divided into two phases (Figure 4). The first phase is the initial stage. It corresponds to rapid dissolution, with high dissolution rate over the first 40 min. This initial phase can be attributed to the dissolution of very fine or / and highly reactive carbonate minerals (example euhedral or subhedral minerals) with influencing significantly the overall dissolution rate. In the second phase (from 40min to 100min), the dissolution rate decreases which is the steady stage. This second phase corresponds to slower dissolution. This abrupt drop of dissolution rate suggests that most of unstable and reactive minerals have been dissolved, therefore, the carbonate rocks tend to be stable.

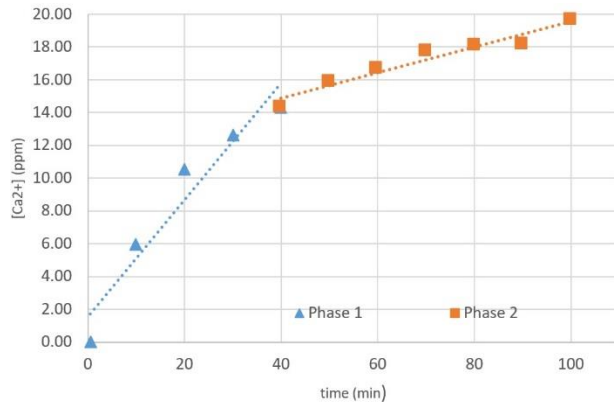


Fig. 4. Example of dissolution model showing two phases of dissolution with different dissolution rate

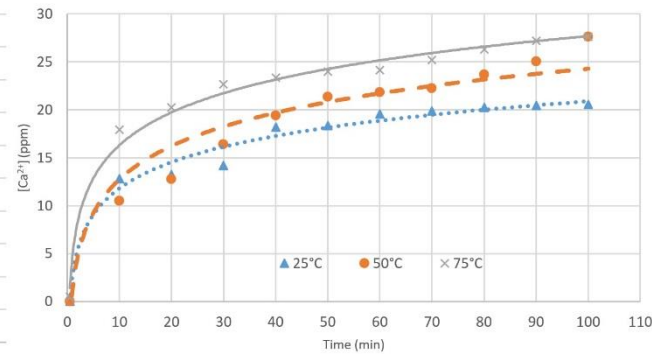


Fig. 5. Dissolution kinetic model at 75°C, 50°C, and 25°C

Dissolution kinetic of carbonate is temperature dependent [6-7]. From the analysis of dissolution kinetic models, the dissolution rate is proportional to the temperature. Therefore, samples belonging to the same facies and dissolved at 75°C exhibit the highest dissolution rate and the others dissolved at 25°C show the lowest dissolution rate (Figure 5).

At 25°C, boundstone is the microfacies showing the highest dissolution with mean dissolution rate of 3.95 ppm /min. On the other hand, grainstone and wackestone is characterized by similar models with overlapping dissolution curves (Figure 6). Figure 6

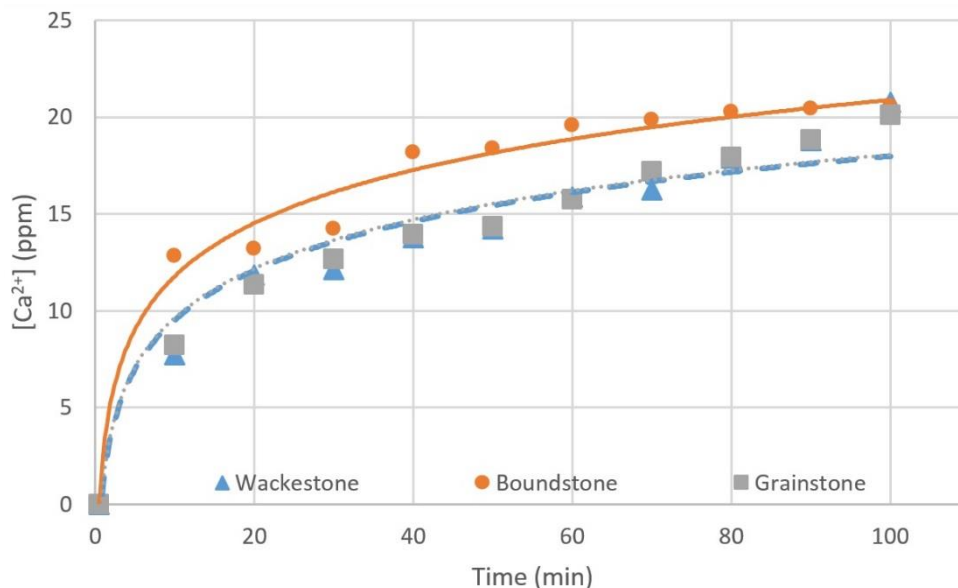


Figure 6. Dissolution model of the three microfacies at 25°C

At 50°C and 75°C, boundstone still exhibits the highest dissolution rate. The wackestone and the grainstone have similar dissolution models (Figures 7a and 7b). However, wackestone dissolves faster than the grainstone because wackestone consists of larger pore sizes.

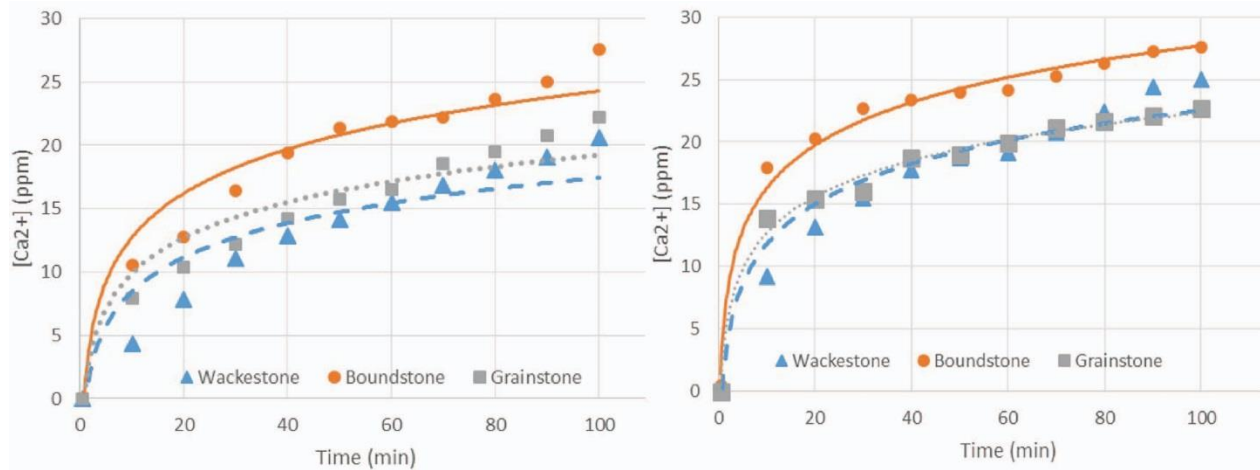


Figure 7. Dissolution model of the three microfacies at a - 50°C; b-75°C

Among the studied microfacies at a given temperature, boundstone is the microfacies with the highest dissolution rate, followed by wackestone and grainstone. Therefore, based on mean dissolution model of each microfacies, it can be interpreted that the dissolution rate is related to porosity, permeability and crystal size.

3.3. Modeling the impact of petrophysical and textural parameters

Stepwise multiple regression analysis [8-9] is the adopted statistical method used to evaluate the impact of porosity, permeability and crystal sizes on dissolution kinetic models at different temperature.

At 25°C, the developed model shows a strong correlation ($R^2= 0.86$) with its dependent variables. However, based on significance (sig) value or p-value, permeability is not significant for the model (p-value or sig = $0.42 > 0.05$). Therefore, the best model is defined by equation (2).

$$[Ca^{2+}] = f(t, \Phi, K, CS) = 0.14t + 16.15\Phi - 0.17CS + 4.2 \quad (2)$$

The confidence level at 95% for each parameter and their significance are summarized in table 2. This results show that time and porosity have positive effect on released Ca^{2+} whereas the crystal size filling the pores has negative effect on dissolution. The permeability, however, appears to have no impact on dissolution model.

Table 2. Coefficient of variables of dissolution model at 25°C and their significance

Model at 25°C ($R^2=0.86$)	Coefficients B	Sig.	95% Confidence Interval for B Lower Bound	Upper Bound
(Constant)	4.271	0	2.756	5.785
Time (t)	0.137	0	0.124	0.151
Porosity (Φ)	16.15	0	10.973	21.327
Permeability (K)		0.42		
Crystal size (CS)	-0.017	0.003	-0.027	-0.006

At 50°C, the dissolution model is defined by equation (3) and also depends on time, porosity and carbonate crystal size filling the pores with moderate correlation ($R^2=0.65$). However, permeability is not significant (sig = $0.93 > 0.05$). This is consistent with the model at 25°C (Table 3).

Table 3. Coefficient of variables of dissolution model at 50°C and their significance

Model at 50°C ($R^2= 0.65$)	Coefficients B	Sig.	95.0% Confidence Interval for B	
			Lower Bound	Upper Bound
(Constant)	4.1	0.014	0.847	7.352
Time (t)	0.165	0	0.135	0.194
Poro(Φ)	18.866	0	8.756	28.975
Permeability (K)		0.93		
Crystal size (CS)	-0.037	0.003	-0.061	-0.013

$$[Ca^{2+}] = f(t, \Phi, K, CS) = 0.17t + 18.87\Phi - 0.04CS + 4.1 \quad (3)$$

At 75°C, the dissolution model is described by equation (4) and is also in agreement with the models at 25°C and 50°C with a moderate correlation ($R^2=0.56$). The porosity and permeability has a positive effect on the dissolution kinetic whereas crystal sizes reduce the rate of dissolution (Table 4). Permeability does not contribute to the enhancement or reduction of dissolution rate in carbonate rocks ($sig=0.1 > 0.05$).

$$[Ca^{2+}] = f(t, \Phi, K, CS) = 0.13t + 17.87\Phi - 0.03CS + 10.38 \quad (4)$$

Table 4. Coefficient of variables of dissolution model at 75°C and their significance, Model validation and testing

Model at 75°C ($R^2= 0.56$)	Coefficients B	Sig.	95% Confidence Interval for B	
			Lower Bound	Upper Bound
(Constant)	10.379	0	7.018	13.739
Time (t)	0.125	0	0.094	0.156
Poro (Φ)	17.816	0.001	7.784	27.848
Permeability (K)		0.1		
Crystal size (CS)	-0.033	0.007	-0.057	-0.009

In order to validate the dissolution model as a function of time, porosity and crystal size, measured $[Ca^{2+}]$ data from the dissolution experiment are plotted against predicted data from the 25°C model (Figure 8a), 50°C model (Figure 8b) and 75 °C model (Figure 8c).

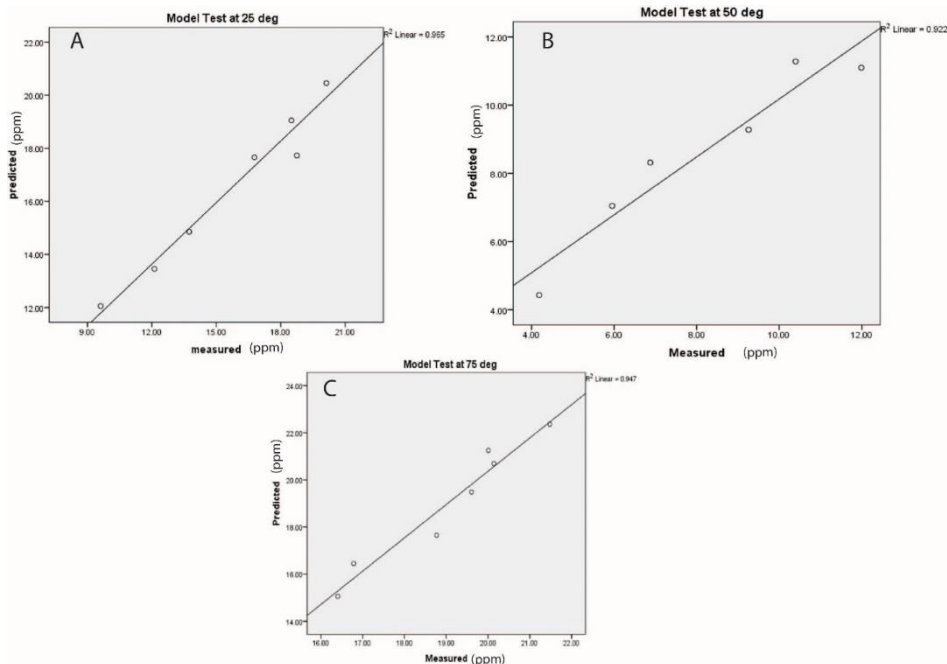


Figure 8. Crossplot between measured and predicted $[Ca^{2+}]$ released in the system at a- 25°C, b-50°C; c-75°C

4. Conclusion

Dissolution of three carbonate microfacies (wackestone, grainstone and boundstone) have been modeled at different temperatures (25°C, 50°C and 75°C) in order to evaluate the effects of petrophysical and textural parameters on dissolution. The experiment was conducted under controlled conditions inside a reactor chamber. For each temperature, the general dissolution model as a function of time is described by log-linear function with the slope representing the dissolution rate. The dissolution model has two phases, the rapid initial phase from 0-40min and the slow steady phase from 40-100min.

The dissolution kinetics expressed through dissolution rate is proportional to temperature. Therefore, carbonate dissolved at higher temperature dissolves faster than carbonate dissolved at lower temperature regardless of carbonate microfacies. Taking into account the texture of each microfacies, the dissolution of boundstone is faster than the dissolution of grainstone and wackestone. The dissolution models for grainstone and wackestone are similar with overlapping curves at a given temperature due to similar crystal sizes.

Different models at three different temperatures were developed based on released $[Ca^{2+}]$ as function of dissolution time, porosity, permeability and pore-filling crystal size. The three models shows that dissolution depend on time and porosity which positively affects dissolution. These models are also function of carbonate crystal size filling the pores. Larger crystal sizes cause a reduction in dissolution rate. Permeability appears not to have a significant impact on the dissolution kinetic model.

Acknowledgment

This study is supported by YUTP grant awarded to E. Padmanabhan.

List of symbols

$[Ca^{2+}]$	Concentration of calcium ion (Ca) released within the system [ppm]
t	time [min]
M	dissolution rate [ppm/min] constant
P	intercept [ppm] constant
Φ	Porosity (ratio)
K	permeability (mD)
CS	Pore filling crystal size (μm)
$Sig.$	Significance
R^2	coefficient of determination
Temp or T	Temperature °C

References

- [1] Plummer LN, Parkhurst DL and Wigley TML. 1979, Critical Review of the Kinetics of Calcite Dissolution and Precipitation. ACS Symposium Series, Vol. 93, Chemical Mode-ling in Aqueous Systems, Chapter 25, pp 537–57.
- [2] Schott J, Brantley S, Crerar D. Guy C, Borcsik M., Willaime C. 1989, Dissolution kinetics of strained calcite: *Geochimica et Cosmochimica Acta*, Vol. 53, p. 373–382.
- [3] Letterman R. 1995, Calcium Carbonate Dissolution Rate in Limestone Contractors: Research and Development Report, EPA/600/SR-95/068, Risk Reduction Engineering Laboratory, Cincinnati, OH.
- [4] Morse JW, and Arvidson RS. 2002, The dissolution kinetics of major sedimentary carbonate minerals: *Earth-Science Reviews*, v. 58, no. 1-2, p. 51–84.
- [5] Dolgaleva IV, Gorichev IG, Izotov AD, and Stepanov VM. 2005, Modeling of the Effect of pH on the Calcite Dissolution Kinetics: *Theoretical Foundations of Chemical Engineering*, 39(6): 614–621.
- [6] Peng C, Crawshaw JP, Maitland GC, and Trusler JPM 2014, Kinetics of Calcite Dissolution in CO_2 -Saturated Water at Temperatures between (323 and 373) K and Pressures up to 13.8 MPa: *Chemical Geology*, p. 1–25.

- [7] Pokrovsky OS, Golubev SV, and Schott J. 2005, Dissolution kinetics of calcite , dolomite and magnesite at 25°C and 0 to 50 atm $p\text{CO}_2$: *Chemical Geology* 217 (3), 239-255.
- [8] Kirkpatrick LA, and Feeney BC. 2009, Multiple Regression, in *A simple guide to SPSS: For version 16.0*. Belmont: Wadsworth, p. 86 to 96.
- [9] George D, and Mallery P. 2005, *Advanced and Regression Modules*, in A. and Bacon, ed., *SPSS for Windows Step by Step*.
- [10] Rumsey DJ. 2016, How to Interpret a Correlation Coefficient r , in *Statistics For Dummies*.

**corresponding author: Spariharijaona Andriamihaja; andriamis@yahoo.fr*